ACS APPLIED MATERIALS & INTERFACES

www.acsami.org

Research Article

Multiblock Copolymers for Recycling Polyethylene–Poly(ethylene terephthalate) Mixed Waste

Keiichiro Nomura, Xiayu Peng, Hanim Kim, Kailong Jin, Hee Joong Kim, Abigail F. Bratton, Christopher R. Bond, Amelia E. Broman, Kevin M. Miller,* and Christopher J. Ellison*

Cite This: https://dx.doi.org/10.1021/acsami.9b20242

Read Online

ACCESS | Metrics & More | Article Recommendations | Supporting Information

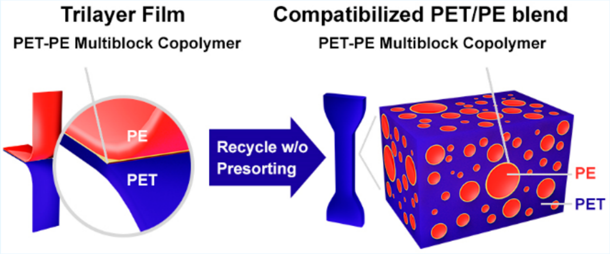

ABSTRACT: Plastic pollution is one of the most pressing global environmental issues we face today, in part due to the continued rise in production and use of disposable plastic products. Polyolefins and polyesters are two of the most prevalent polymers in the world accounting for ∼80% of total nonfiber plastic production. Recycling, despite being intrinsically environmentally friendly and sometimes economically viable, remains at a surprisingly low level (<9% in the U.S.) with most plastic waste ending up in landfills. One reason for this low rate of recycling stems from the challenge of recycling mixed waste streams and multicomponent plastics. In mixed waste streams, physical presorting of components prior to recycling requires significant effort, which translates to added cost. For multicomponent plastics (e.g., multilayer films such as food wrappers), the individual plastic components cannot be efficiently physically separated, and they are immiscible with poor interfacial adhesion when melt reprocessed. Thus, direct recycling of mixed plastics by melt reprocessing results in products that lack desired end-use properties. In this study, we describe the synthesis of novel poly(ethylene terephthalate)–polyethylene multiblock copolymers (PET–PE MBCPs) and evaluate their utility as adhesive tie layers in multilayer films and compatibilizer additives for melt reprocessed blends. PET and PE are targeted because they are two of the most prevalent commercial polymers in the world and are high volume waste streams. The work described here demonstrates two key findings. First, the PET–PE MBCPs serve as effective adhesive tie layers between neat PET/PE films with adhesive strength comparable to that of commercially available adhesives. Second, PET/PE (80/20 wt %) blends containing ∼0.5 wt % PET–PE MBCP were melt mixed to mimic recycling mixed plastic waste, and they were found to exhibit mechanical properties better than neat PET. Overall, this study demonstrates that PET–PE MBCPs could significantly enhance the ability to recycle PET/PE mixed waste streams by serving the role as both an adhesive promoting layer and a compatibilizer additive.

KEYWORDS: *polyethylene, poly(ethylene terephthalate), multilayer, multiblock copolymer, recycling, polymer blends, adhesive, compatibilizer*

■ INTRODUCTION

Polymeric materials are essential to our daily life in packaging, textiles, construction, electronics, and transportation. Many properties of synthetic polymers, such as excellent chemical resistance, strength to weight ratio, and low cost, make them attractive replacements for traditional materials such as metal, glass, wood, and ceramics. These properties have led to growth in the worldwide annual production of plastics to 380 million tons as of 2015.[1] Importantly, about 42% of the total plastic production is used for packaging applications, most of which are single-use before being discarded.[1] Polyesters and polyolefins are commonly used in packaging and are two of the most highly produced and consumed polymers in the world, accounting for ∼80% of total nonfiber plastic production. By design, the majority of synthetic polymers are robust in a range of use environments, and they typically take hundreds of years to degrade.[2] As a result, several serious environmental problems have arisen, such as ocean pollution and microplastic accumulation throughout the food chain.[2−4] In an effort to reduce their environmental impact, polymer recycling and the implementation of degradable substitutes continue to be explored.[4,5] However, among the polymer waste streams in the United States (∼30 million tons annually), only <9% of the total polymer waste is recovered from municipal solid waste for recycling, a large fraction of which is composed of poly(ethylene terephthalate) (PET) and polyethylene (PE).[6,7] PET and PE are used extensively as packaging materials because PE exhibits ductility, impact strength, chemical resistance, heat sealability, and moisture barrier properties, while PET provides superior oxygen barrier

Received: November 7, 2019
Accepted: February 4, 2020
Published: February 4, 2020

properties, thermal stability (up to 350 °C), high modulus, and good mechanical strength.

In food packaging, multilayer films composed of two or more polymers are often used to combine the advantages of the components, thus improving their overall performance. For example, multilayer films containing PET/poly(vinylidene dichloride)/PE with thickness ratio of 25/5/70 are used in processed meat (e.g., ham) packaging.[8] Given that most polymer combinations (such as PET/PE) are inherently immiscible, their processing into adjoining layers results in relatively sharp interfaces between the layers and poor interlayer adhesion. Numerous attempts have been made to improve adhesion between different polymer layers, and they can be classified into two categories. One approach involves adding an intermediary polymer adhesive layer called a tie layer that can be used between the two different homopolymer layers.[9−15] Tie layer polymers usually have functional groups, such as maleic anhydrides or glycidyl (meth)acrylates, which are grafted or randomly introduced into tie layer copolymers. A tie layer copolymer can chemically react with one or both layers so the two layers can adhere effectively via covalent bonds. Alternatively, the copolymer can participate in secondary bonding, such as hydrogen bonding, to enhance adhesion. One prominent example is reactive polyurethane adhesives that contain residual reactive functional groups, such as isocyanates (e.g., from toluene diisocyanate, diphenylmethane diisocyanate, etc., precursors) and hydroxyls (e.g., from poly(ethylene glycol), poly(propylene glycol), etc., polyol precursors) that can react with adjoining layers, in addition to the possibility of secondary interactions facilitated by their repeat unit structures. The second approach involves surface modification by ion sputtering, corona irradiation, or plasma irradiation.[16−19] These treatments enhance the surface properties of polymer films to promote adhesion by chemical (i.e., functional group modification) and physical (i.e., roughening) modification of the surface.

While PET and PE are recyclable in neat form, PET/PE multilayer films are extremely challenging, if not impossible, to recycle since the pure components cannot be physically separated from each other due to the adhesion promoted by the tie layer.[20] Because economics, processability, and performance are the main driving forces for the structure and selection of materials, most multicomponent products are prepared with little or no consideration for their recyclability.[21] The easiest and most economical way of recycling these multicomponent systems is to simply melt reprocess them after their intended use. However, the resulting melt reprocessed/recycled blends usually possess poor mechanical properties due to previously mentioned immiscibility issues. To achieve recycled blends consisting of PET and PE with desirable mechanical properties, compatibilizer additives are typically required. For instance, it is known that random, block, and graft copolymers[22−28] containing chemical units that either (1) interact strongly with or (2) resemble the primary polymer blend components are often suitable compatibilizers because portions of the compatibilizer are then partially or completely miscible with each blend component.[22] If designed appropriately, compatibilizers can migrate to and localize at the interface between the two blend components, often resulting in a concomitant decrease in interfacial energy and enhancement in interfacial adhesion between the immiscible blend polymers. As a result, compatibilized blends usually consist of a minority polymer phase that is finely dispersed (e.g., spherical domains a few micrometers in average diameter or smaller) in a majority matrix second polymer phase with compatibilizers localized at the interfaces. All of these factors enhance the macroscopic mechanical properties of immiscible blends such that they are in between those of the neat homopolymer blend components, analogous to the behavior of miscible blends.[22]

It is noteworthy that compatibilizer and tie layer polymers are different, although their chemical structures can be similar in some instances. Tie layer polymers are primarily designed as intermediary layers for improving interlayer adhesion in multilayer film without consideration for their potential compatibilization capabilities in an immiscible blend. Any given tie layer polymer may be a suitable blend compatibilizer and any given blend compatibilizer may be a suitable tie layer, but the mechanistic details defining performance are different. For example, a tie layer polymer is not required to migrate to an interface as for compatibilizers in blends. While compatibilizers are usually monolayers self-assembled at the interface between homopolymers, tie layers are typically thicker due to their direct application, often through lamination during film processing; however, tie layer and compatibilizer polymers can both promote adhesion between two immiscible polymers.

The simplest approach to compatibilization of PET/PE blends involves addition of nonreactive, preformed additives.[29−33] For example, through the addition of 5−20 wt % styrene−ethylene-*co*-butene−styrene (SEBS) triblock copolymer (TBCP) to PET/high-density PE (HDPE) blends (75/25−25/75 wt %), improvements in the ductility of the ternary blends were reported by Traugott et al. and Barlow et al.[30,31] The strain at break for a PET/HDPE (75/25) blend film with addition of 20 wt % SEBS was 3 times that compared to blends without SEBS. The authors hypothesized that the PS block in SEBS acted as a PET-like block whereas the PEB block acted as a PE-like block promoting localization of SEBS at the interface to compatibilize the PET and PE. Interestingly, the PS block is not miscible with PET, and the PEB block is not expected to be miscible with HDPE. Not surprisingly, significant improvements in ductility required high compatibilizer loadings of more than 10 wt %, which significantly depressed the modulus.

Alternatively, other research has investigated compatibilization of PET and PE (HDPE, linear low-density PE (LLDPE), or low-density PE (LDPE)) blends by introducing reactive PE additives with different types of functional groups (e.g., maleic anhydride, glycidyl, or amino functional groups). This strategy envisions that the functional PE additive will react with PET at the interface during melt mixing to form a compatibilizer in situ.[32−44] In these works, more than 5 wt % of the reactive additives are added to obtain a compatible blend. Recently, Todd et al. synthesized a *tert*-butyloxycarbonyl (BOC) protected amino-telechelic PE additive (i.e., functionalized at both chain ends), which was melt mixed with PET/HDPE (90/10 wt %) blends.[47] The BOC protected amino-telechelic PE additive underwent thermolysis to produce an amino-telechelic PE additive that enabled reaction with PET homopolymer. This reaction was hypothesized to promote formation of multiblock copolymers (MBCPs) in situ. Remarkably, just 0.5 wt % of the functionalized PE additive was effective at compatibilization evidenced by an 8-fold reduction in dispersed HDPE particle size and a 12-fold increase in the strain at break nearing that of PET. Unfortunately, it was not possible to verify the amount or molecular architecture of the formed compatibilizer because it was not isolated. In addition, a relatively long melt mixing residence time (~10 min) was required for the reaction to occur, and the reaction byproducts (carbon dioxide and isobutylene) could be a concern for forming voids in the blend product if they volatilize during melt mixing. Regardless, the suggestion by this study that compatibilization of PET/PE blends with MBCPs may be possible at exceedingly low loadings is highly attractive.

As compared to traditional diblock copolymers (DBCP)s or symmetric TBCPs as preformed compatibilizers, MBCPs composed of two block types with more than three overall blocks exhibit advantages in compatibilization and improving interfacial adhesion.[24] Eastwood and Dadmun found that polystyrene/poly(methyl methacrylate) (PS/PMMA) bilayer films loaded with PS−PMMA pentablock copolymer in between showed greater interfacial toughness compared to PS−PMMA DBCP or TBCP.[48] Recently, Eagan et al. and Xu et al. reported the synthesis of ethylene and isotactic propylene (PE−*i*PP) MBCPs.[49,50] Interfacial adhesion between *i*PP and PE films was significantly improved with PE−*i*PP tetrablock copolymers in between compared to analogous DBCPs. Furthermore, PE/*i*PP blends with ≤1 wt % MBCP compatibilizer exhibited attractive mechanical properties in between those of the neat blend components, suggesting the ductile blends could be used in recycled products.

To address the critical need to recycle polyolefin−polyester mixed waste, here we focus on one of the most important waste mixtures composed of PET and PE. PET−PE MBCPs were synthesized for the first time with the objective of improving interfacial adhesion, mechanical strength, and compatibility in *both* PET/PE multilayer films and blends. Generally, this task is difficult as PET and PE have a very large positive Flory−Huggins interaction parameter ($\chi_{\text{PET-PE}} = 0.41$) (described in the Supporting Information in detail), confirming they are highly incompatible, possess few common good solvents, and exhibit thin interfacial thicknesses that result in very poor interfacial adhesion without additives. MBCPs were prepared by coupling hydroxy-terminated PET and PE precursors through a polyesterification reaction. Interlayer adhesion of multilayer films containing MBCPs was evaluated by peel tests, and the mechanical properties and morphology of PET/PE/MBCP blends were analyzed by using uniaxial tensile tests and scanning electron microscopy (SEM), respectively. Ultimately, this research seeks to improve the recyclability of this commercially important mixed waste stream into blend products.

■ RESULTS AND DISCUSSION

Synthesis and Characterization of Block Copolymers.

PET−PE MBCPs were synthesized via a coupling reaction between dihydroxy-terminated PET and PE precursors with terephthaloyl chloride. Acid chlorides have recently been employed by Panthani et al. in the preparation of poly(lactide-*b*-butadiene-*b*-lactide) and poly(lactide-*b*-ethylene-*co*-ethyl ethylene-*b*-lactide) MBCPs.[51,52] Targeted PET precursors ($M_n \approx$ 4 kg/mol or 7 kg/mol) were obtained via step-growth solution polymerization of ethylene glycol and terephthaloyl chloride in tetrahydrofuran (Figure S1). Dihydroxy-terminated PE precursors ($M_n \approx$ 4 kg/mol or 7 kg/mol) were obtained via ring-opening metathesis polymerization (Figure S2) as described elsewhere.[53,54] Characterization data of the PE and PET precursors are summarized in Table 1. MBCP-4k and MBCP-7k were then synthesized from PET-4k/PE-4k and PET-7k/PE-7k, respectively, with terephthaloyl chloride (1:1 hydroxy:acid chloride functional group ratio to produce MBCPs that are roughly 50:50 PET:PE by mass) as a coupling agent in 1,1,2,2-tetrachloroethane (TCE) at 120 °C (Figure 1). It is noteworthy that there are very few solvent choices for solubilizing this pair of dihydroxy precursors. Melt state coupling may be possible, but detailed synthetic investigations were outside the scope of this study.

Table 1. Characterization and Properties of BCP Precursors

precursor	M_n(^{1}H NMR) (g/mol)	M_n(SEC)[c] (g/mol)	$Đ$[c] (M_w/M_n)	T_m[d] (°C)
PET-4k (dihydroxy-terminated)	4600[a]			251
PET-7k (dihydroxy-terminated)	7100[a]			238
PE-4k (dihydroxy-terminated)	4400[b]	4300	2.72	129
PE-7k (dihydroxy-terminated)	6600[b]	6400	2.53	130
monoPE-4k (monohydroxy-terminated)	4600[b]	4100	1.09	107

[a] Determined by ^{1}H NMR spectroscopy in 8:1 chloroform-*d*/trifluoroacetic acid-*d* at 25 °C. [b] Determined by ^{1}H NMR spectroscopy in TCE-d_2 at 120 °C. [c] Determined by SEC in 1,2,4-trichlorobenzene at 135 °C compared with PS standards via universal calibration with appropriate Mark−Houwink parameters. [d] Determined by second heating of DSC results with a heating rate of 5 °C/min (Figure S3a).

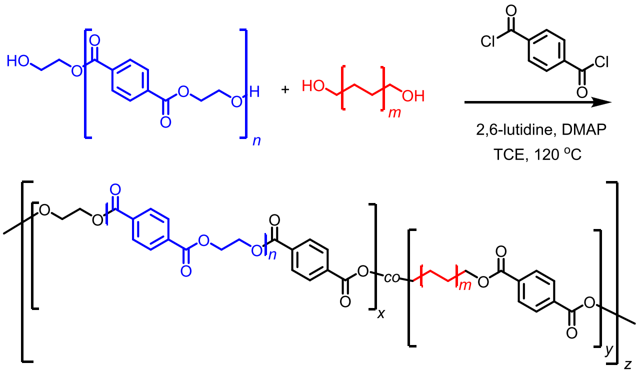

Figure 1. Synthetic scheme for the preparation of PET−PE MBCPs.

From proton nuclear magnetic resonance (^{1}H NMR) spectroscopy, the near-full conversion of precursors into MBCPs was confirmed by the significant reduction of end-group peaks from the block precursors. With the synthetic scheme used in this study, the self-coupling of polymer precursors could not be completely eliminated, meaning the block sequencing in the MBCP is essentially random. The molecular weights (MWs) of the MBCPs were evaluated by ^{1}H NMR spectroscopy (Figure S4) via end-group analysis (described in the Supporting Information in detail), the results of which are summarized in Table 2. From the calculated M_n values, it was determined that MBCP-4k contained about 10 blocks on average, while MBCP-7k was found to have about 13 blocks on average. A distribution in total number of blocks per chain is expected but difficult to characterize absolutely. As the MBCPs do not dissolve in common size exclusion chromatography (SEC) solvents, this method could not be employed in a

https://dx.doi.org/10.1021/acsami.9b20242

Table 2. Characterization and Properties of PET−PE BCPs

polymer	M_n[a] (g/mol)	T_m[b] (°C)	f_{PET}[c]	f_{PE}[c]
MBCP-4k	45500	124, 250	0.42	0.58
MBCP-7k	90200	127, 253	0.41	0.59
TBCP	14900	105, 242	0.31	0.69

[a] Determined by ^{1}H NMR spectroscopy in TCE-d_2 at 120 °C. [b] Determined by second heating of DSC thermogram with a heating rate of 5 °C/min. [c] Determined by ^{1}H NMR spectroscopy according to the melt density of PET and PE (0.989 and 0.769 g/cm^3, respectively[55]).

traditional manner. Rather, MBCPs were dissolved in TCE at 135 °C, and then the solution was injected into the trichlorobenzene (TCB) mobile phase at 135 °C. Broad, nearly symmetric, monomodal chromatograms were obtained for all the synthesized MBCPs, and a clear shift to shorter retention time was observed from their corresponding PE and PET precursors. Knowing that dn/dc for PET is positive under these conditions, while that of PE is negative, these data suggest there is little residual unreacted PET precursor in the MBCPs (Figure S5). Assessment of the thermal properties of the MBCPs by DSC (differential scanning calorimetry) indicated two melting transitions (T_m) for crystalline PET (ca. 250 °C) and PE (ca. 125 °C) (Table 2 and Figure S3b) domains, respectively. A PE−PET−PE TBCP was synthesized for comparison. In short, the 4k hydroxy-terminated PET oligomer was reacted with a large excess of terephthaloyl choride. The resulting diacid chloride-terminated PET oligomer was isolated in a glovebox and then reacted with 2 equiv of 4k monohydroxy-terminated PE oligomer which was synthesized by anionic polymerization. (Figures S6 and S7) Additional synthetic details can be found in the Supporting Information. We were unable to identify efficient synthetic pathways to make a symmetric diblock copolymer or a PET−PE−PET TBCP. The properties of the precursors and the BCPs are provided in Tables 1 and 2, respectively. The obtained BCPs were confirmed to be stable at 270 °C by thermogravimetric analysis (Figure S8).

Interfacial Adhesion of PET/BCP/PE Trilayer Film. To evaluate interfacial adhesion, T-peel tests of laminates was performed. Trilayer films were prepared by sandwiching a spin-coated thin layer of the BCP in between PET and PE layers (Figure S9). In this study, LLDPE film was selected as the model PE film, which is widely combined with PET and used in multilayer films. LLDPE exhibits a good balance of moisture barrier and thermal resistance characteristics while preserving heat sealability. We acknowledge that commercial multilayer films are usually more complicated than a simple trilayer structure. However, we have focused on the trilayer structure to prove the concept with the expectation that future studies will need to evaluate its effectiveness in other multilayer structures. To image the cross sections of the trilayer laminate films, atomic force microscopy (AFM) was utilized. Shown in Figure 2a and Figure S10 are representative cross-sectional images of trilayer laminates after microtoming where MBCP-4k was employed as the interlayer. In general, the thicknesses of the TBCP, MBCP-4k, and MBCP-7k interlayers used here were determined to be 240, 220, and 290 nm, respectively. For comparison, the periodic domain spacing (D) of the bulk TBCP, MBCP-4k, and MBCP-7k was estimated as 23.7, 27.3, and 34.0 nm, respectively, by small-angle X-ray scattering (SAXS) at 270 °C (Figure S11 and Table S1). This indicates the total MBCP interlayer thickness in the laminates was at least 8−10 times D. Taking MBCP-7k as an example, there are an average of 13 blocks per chain (equivalent to 6−7 domain periods D), suggesting it is not possible for a single MBCP chain to span completely from the PET layer to the PE layer. However, the MBCPs have a relatively broad MW distribution due to the nature of their synthesis by coupling functional groups, introducing the possibility that some fraction of the MBCP polymer chains (i.e., MBCPs with more than 20 blocks with additional consideration for bridging versus looping configurations) may be able to reach from the PET layer to the PE layer while the TBCP obviously cannot.

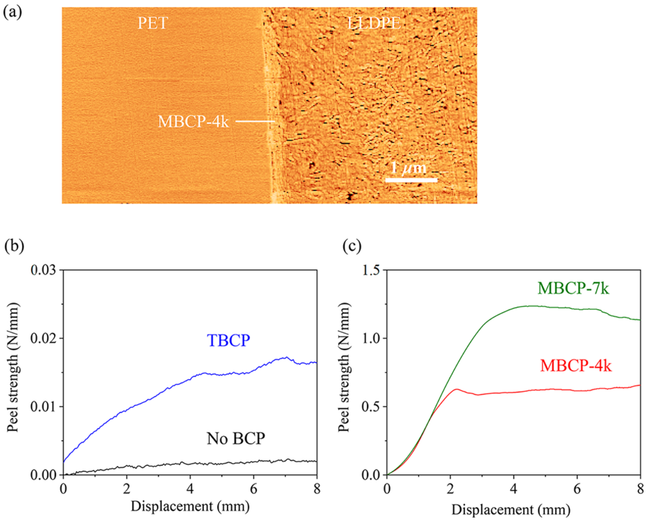

Figure 2. Structure and peel strength of trilayer laminate films. (a) AFM phase image of PET/MBCP-7k/PE laminate cross section. Representative peel strength curves from PET/PE laminates, (b) without BCP and with TBCP, and (c) with MBCPs composed of two different precursor MWs. The individual peel strength curves are provided in Figure S12.

For the T-peel test, typical data exhibit an initial rise in peel strength at the start of the experiment followed by the more important plateau value at steady state that is the focal point here (Figure 2b,c). Figure 2b shows peel test results from a "control" PET/PE bilayer laminate film (no BCP) that indicates very little adhesion of $(1.73 \pm 0.59) \times 10^{-4}$ N/mm (average and standard deviation from three repeated tests). The average peel strengths were calculated by using the displacement range of 4−8 mm. As mentioned previously, bilayer films composed of only PET and PE are expected to exhibit poor interfacial adhesion without an intermediate tie layer or surface treatment due to their high incompatibility and thin interfacial thickness. The interfacial thickness a_I between the two immiscible polymers over which the repeat units are compositionally mixed can be estimated by the following equation:[56]

$$a_I = 2\sqrt{\frac{(b_1{}^2 + b_2{}^2)}{12\chi}}$$

where χ is the Flory−Huggins interaction parameter and b is the statistical segmental length. The χ_{PET-PE} at 270 °C was calculated to be 0.41 with a statistical segmental length of b_1 = 7.9 Å (PET) and b_2 = 8.4 Å (PE)[57] (described in the Supporting Information in detail). The interfacial thickness of PET/PE was calculated as 10.4 Å, which is around one-fourth

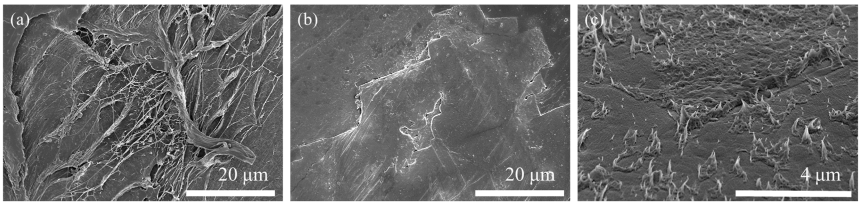

Figure 3. Representative SEM micrographs of failure surfaces after peel testing (a) LLDPE layer from PET/MBCP-4k/LLDPE films, (b) PET layer from PET/MBCP-4k/LLDPE films, low magnification, and (c) PET layer from PET/MBCP-4k/LLDPE films, observed with 70° tilted sample stage, high magnification.

of the value estimated for the *i*PP/PE system ($a_I \approx 40$ Å) that also exhibits poor adhesion.[50,58] The reduction in interfacial width is consistent with the higher incompatibility of the PET/PE system. Thinner interfaces generally reduce the amount of interpenetration and mixing between two adjoining polymers, resulting in lower interfacial adhesion.

On the other hand, PET/BCP/PE trilayer laminate films exhibited moderate to substantial increases in adhesion. When the TBCP interlayer was utilized, the adhesive strength increased to $(1.36 \pm 0.37) \times 10^{-3}$ N/mm, nearly 4 times higher than the control. Furthermore, the adhesive strengths in trilayer films with MBCP-4k or MBCP-7k interlayers were 0.62 ± 0.04 and 1.14 ± 0.06 N/mm, respectively, an increase of 2−3 orders of magnitude over the control, comparable to or exceeding those reported for reactive tie layers.[13−15]

The representative failure surfaces after peel tests of trilayer films with MBCP-4k and TBCP as adhesion interlayers were examined with SEM (Figure 3). For the sample with a MBCP-4k interlayer, plastic deformation in the form of elongated fibrils was clearly observed on the LLDPE failure surface (Figure 3a). While on the PET failure surface, there was no clear plastic deformation at low magnification (Figure 3b), but residual large film-like patches of the MBCP film remain. Because the peel tests were performed well below the glass transition temperature of PET and cocrystallization between the PET film and PET portions of the MBCP is unlikely due to the rapid thermal quench applied during sample preparation which nearly eliminates PET crystallization (Table S2 and Figure S14), large-scale plastic deformation is not expected at this surface. From the micrograph with higher magnification and tilt view (Figure 3c), we observed residual small patches of MBCP that look like they have undergone significant deformation. These results suggest that there were combined adhesive and cohesive failures. In contrast, the failure surfaces of trilayer films with TBCP as the adhesive interlayer were smooth as shown in Figure S13, which is consistent with low adhesive strength.

There are several important factors that affect the resulting interfacial adhesion such as miscibility of the blocks in the BCP interlayer with each homopolymer layer, molecular entanglements between layers, and cocrystallization. In this system, the PET block is molecularly identical and miscible with the PET homopolymer layer. The PE block in the BCP is molecularly identical to HDPE, which is miscible with the LLDPE used here with a branch content of ∼40 CH_3/1000 C.[59,60] This miscibility maximizes the amount of interpenetration/intermixing between the blocks of the BCPs and the adjoining homopolymer layers, which in turn can promote entanglements and cocrystallization. It is also possible that the interfacial thickness between the homopolymer layers and the BCP interlayers could be even more broadened compared to the PE/PET bilayers in the absence of BCPs. For example, interfaces between PS/PMMA homopolymers exhibited significant broadening (∼50% by neutron reflectivity) in the presence of PS−PMMA DBCP due to the penetration of the BCP adhesive layer into the adjoining homopolymer phases.[61] Similarly, we believe that the PET and PE blocks in the BCPs studied here penetrate into and expand their compositionally mixed interfacial regions. The use of MBCPs rather than the TBCP allows for more interfacial crossing due to a larger number of individual PET and PE blocks which could enhance this effect.

As for entanglements, it is well-known that there is a critical molecular weight (M_c) necessary to significantly improve adhesion, and the M_c is generally 2−3 times that of the entanglement molecular weight (M_e; M_e = 1170 g/mol for PET and 828 g/mol for PE).[57,62] Data reported by Zhang et al. support the notion that insufficient MW promotes adhesive failure by chain pull-out rather than chain scission; entanglements induce failure due to chain scission by serving as molecular barriers to whole chain movement during deformation.[63] Given that the MW of each block in the BCP utilized in this study was above 4000 g/mol and significantly higher than their respective M_c values, it is expected that the necessary MW to improve interfacial adhesion through entanglements has been achieved. Additionally, it is reasonable to expect that the MBCPs used here with 10−13 blocks form entangled loops that anchor within the homopolymer layers.[50] Note that only the middle block in TBCPs can form these anchored entangled loops while DBCPs cannot form them at all. From the adhesion data of MBCP-4k and TBCP, and their failure surface images in Figure 3 and Figure S13, it is clear that the number of blocks greatly affects the interfacial adhesion through the mechanism mentioned above. In addition, by comparing the 4k and 7k MBCP adhesion data, it is evident that an increase in the MW of the individual blocks enhances adhesion, most likely through improvements in both number of interfacial crossings and number of entanglements per MBCP chain.

Finally, the cocrystallization of the MBCPs with their respective homopolymers near the interface should be considered. Xu et al. argued that the radii of gyration of MBCP blocks should be at least larger than the amorphous interfacial thickness between homopolymers, thus enabling the MBCPs to reach crystalline domains of PE and *i*PP homopolymers.[50] We hypothesize that cocrystallization also takes place in this study between the MBCPs and PET and PE layers. Because the interfacial thickness between PET and PE (10.4 Å) where compositional mixing occurs is 4 times thinner than that between *i*PP and PE (40 Å), we estimate that the amorphous interfacial thickness will be proportionally thinner in the PET/PE system (∼2.5 nm) compared to *i*PP/PE (∼10

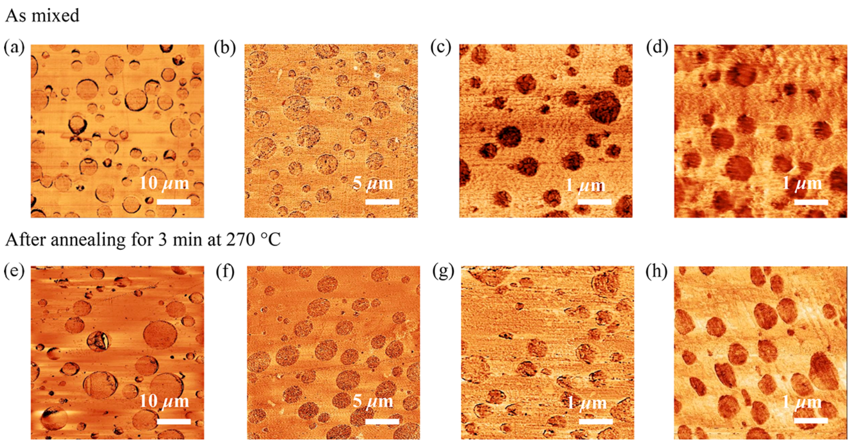

Figure 4. Representative AFM phase images of polymer blends: (a, e) PET/PE (80/20), (b, f) PET/PE/MBCP-4k (80/20/0.5), (c, g) PET/PE/MBCP-4k (80/20/2), and (d, h) PET/PE/MBCP-7k (80/20/2). The D_n of PE in each polymer blend is reported in the text and Table S3.

nm). Through a simple calculation assuming that the radii of gyration of MBCP blocks are equal to the amorphous interfacial thickness (see the Supporting Information for details), the minimum MWs for PET and PE blocks to spatially reach crystallizing regions to cocrystallize with corresponding homopolymers were estimated as 4000 and 3000 g/mol, respectively. These small values are not surprising, considering that PET and PE are a pair of polymers far more immiscible than PE and *i*PP. Because LLDPE and HDPE can cocrystallize,[59] cocrystallization could take place at the interface of the LLDPE layer and the PE block (structurally analogous to HDPE) with MBCP MWs larger than 3000 g/mol. In contrast, cocrystallization is not expected for the PET side since the PET was almost completely amorphous, as confirmed by DSC data (Figure S14 and Table S2), due to the rapid thermal quench applied during sample preparation. Longer MBCP block lengths could further enhance adhesion by promoting additional cocrystallization in the PE phase; these details will be investigated in a future study.

Structure of the Polymer Blends. To mimic the recycling of PET/PE mixed waste and enable effective evaluation of compatibilization, polymer blends composed of neat PET/PE (80/20 by weight) and PET/PE/BCP (80/20/2) were melt mixed in a twin-screw batch mixer. Because PET assumes the role of a rigid and stiff material in PET/PE blends while the rubbery PE can toughen the blend, blends with a PET majority phase were prepared as the resulting properties are more attractive than other alternatives. The addition of block copolymer did not affect the melting temperature of either homopolymer (Figure S15), suggesting that no inter- or transesterification between the BCPs and the homopolymers occurred. The resulting blends were cryomicrotomed, and the remaining smooth surface was imaged by AFM. The AFM phase images shown in Figure 4 and Figure S16 appear with a PET matrix as a lighter color while the PE droplets are darker in color. The contrast comes from the difference in energy dissipation of two different phases. The diameter of each PE droplet (D_i) in the PET matrix was obtained by measuring its cross-sectional area (A_i) with ImageJ software and by using $D_i = 2\left(\frac{A_i}{\pi}\right)^{1/2}$. The number-averaged diameter of all PE droplets was then calculated by $D_n = \sum n_i D_i / \sum n_i$, where n_i is the number of droplets with diameter D_i from more than 30 droplets. The "as mixed" neat blend in Figure 4a shows a D_n value of 3.1 μm compared to 2.5 μm for the blend with TBCP in Figure S16a, indicating a marginal reduction with 2 wt % TBCP. In contrast, the blends with 2 wt % MBCP-4k or MBCP-7k in Figure 4 exhibited D_n values of 0.37 and 0.41 μm, respectively, a significant reduction more than 7 times smaller than the neat blend. Even loadings of 0.5 wt % of MBCP-4k reduced the droplet size more significantly (1.4 μm, Figure 4b) compared to blend with 2 wt % TBCP (2.5 μm). The major conclusion from this "as mixed" blend data is that the MBCPs appear to efficiently migrate, through convective mixing and diffusion in the melt, to locate at the domain interfaces facilitating major reductions in the minority domain size; these are characteristics of a good compatibilizer.

Static/quiescent thermal annealing of the "as mixed" blends was also performed. These tests are important in that they mimic a pelletized melt reprocessed/recycled blend that is then being processed (i.e., by rotational molding or injection molding) into a final form. After static annealing for 3 min at 270 °C, the blend morphology was examined, and the corresponding results are shown in Figure 4e−h and Figure S16c,d. The droplet sizes increased after static annealing in both the neat (from 3.1 to 4.1 μm) and TBCP (from 2.5 to 3.2 μm) containing blends. In contrast, the morphology appears to be essentially unchanged after annealing the blends containing MBCPs (from 1.4 to 1.5 μm for 0.5 wt % MBCP-4k; from 1.0 to 1.2 μm for 1 wt % MBCP-4k; from 0.37 to 0.42 μm for 2 wt % MBCP-4k; and 0.41 to 0.42 μm for 2 wt % MBCP-7k). The results indicate that the MBCPs are more effective at stabilizing the structure than TBCP. Previous studies have shown that simple DBCPs can prevent coalescence of droplets in polymer blends during thermal annealing,[64] with the interfacial energy and interfacial coverage of BCP controlling the coarsening rate. Noolandi further suggested that MBCPs can more easily adopt a pancake shape at the interface between two incompatible homopolymers due to many possible interfacial crossings per MBCP chain, which more efficiently covers the interface than the dumbbell-shaped conformation formed by analogous DBCPs or TBCPs.[65] Balazs et al. and Corsi et al. further supported the idea that MBCPs are readily spread out along the interface of immiscible blends compared to DBCPs and that this structure better facilitates reductions in interfacial energy and steric stabilization against droplet coarsening.[66,67] Therefore, it seems likely that the PET−PE MBCPs expand along the interface, working more efficiently as a compatibilizer in reducing domain size and the coarsening rate compared to TBCP. It is also possible that the MBCPs have higher overall surface coverage at the domain interfaces compared to TBCP. Further research revealing how much MBCP is at the interface compared to inside the homopolymer phases as micelles is necessary to confirm this hypothesis.

Mechanical Properties of the Blends. Mechanical properties of the PET/PE/BCP blends were evaluated by uniaxial tensile tests. Representative stress−strain curves are shown in Figure 5, and the resulting mechanical property values are summarized in Table 3. The Young's moduli of the blends are all similar regardless of BCP type or loading. This is an important feature for effectively compatibilized blends. On the other hand, there were large differences in strain at break. As expected, the neat blend of PET/PE 80/20 was very brittle with about 10% strain at break (Table 3) even though the neat PET and PE parent homopolymers can be extended to more than 200% and 800%, respectively (Figure S18). With the addition of TBCP (2 wt %), the strain at break was observed to increase slightly to 13%. On the other hand, stress and strain at break were dramatically enhanced when MBCPs were added to the blend (Table 3). For example, the strain at break of the blends with the addition of 2 wt % MBCP-4k or MBCP-7k were found to be ∼400%, which is about 40 times better than the neat blend. Significantly, note that only 0.5 wt % of MBCP-4k still improved the strain at break to 333% from 10% for the neat blend. Another important property of a blend material is its toughness, represented by the area under the stress−strain data. The blend samples containing MBCPs all possess toughness greater than that of neat PET, an expected result for a well-compatibilized blend with a rigid PET majority phase and a rubbery PE minority phase, as mentioned earlier. Overall, these results can be explained by efficient localization of the MBCP at the interface between the blend components, making them more stable to melt processing due to the steric stabilization of the minority domain against coarsening. In turn, the same localization improved interfacial adhesion in the solid state to facilitate stress transfer between the PET and PE phases to produce attractive mechanical properties.

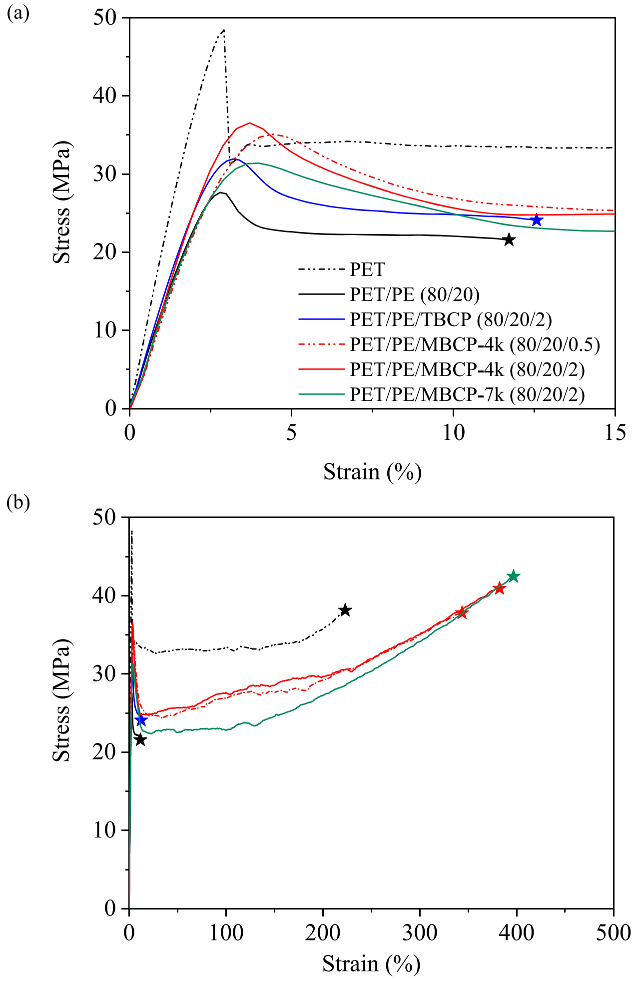

Figure 5. Representative stress−strain curves of PET/PE polymer blends: (a) a magnified view of the low strain region; (b) a view of the full region. The stress−strain curves of individual specimens are provided in Figure S17.

Table 3. Mechanical Properties of PET, PE, and PET/PE Blends (Averages and Standard Deviations from Three Repeated Tests)

polymer	strain at break (%)	stress at break (MPa)	Young's modulus (GPa)
PET	235.6 ± 32.1	39.4 ± 1.1	1.96 ± 0.15
LLDPE	840.4 ± 87.3	24.9 ± 3.4	0.22 ± 0.02
PET/LLDPE(80/20)	9.8 ± 2.3	21.1 ± 1.8	1.28 ± 0.10
PET/LLDPE/TBCP (80/20/2)	13.0 ± 1.5	20.6 ± 5.2	1.40 ± 0.04
PET/LLDPE/MBCP-4k (80/20/0.5)	333.0 ± 93.0	36.2 ± 5.0	1.34 ± 0.10
PET/LLDPE/MBCP-4k (80/20/2)	401.7 ± 18.9	44.0 ± 3.2	1.47 ± 0.06
PET/LLDPE/MBCP-7k (80/20/2)	395.4 ± 21.3	41.9 ± 1.6	1.25 ± 0.02

SEM images of the cryo-fractured PET/PE polymer blends with and without BCPs are shown in Figure 6. Note that the cryo-fracturing process has created large gaps between the two phases in the neat PET/PE blend in Figure 6a, consistent with low interfacial adhesion. These observations are consistent with the previously discussed laminate film peel tests (Figure 2b,c) and the low strain at break during tensile tests. Large PE droplets and cryo-fracture-induced gaps between the two

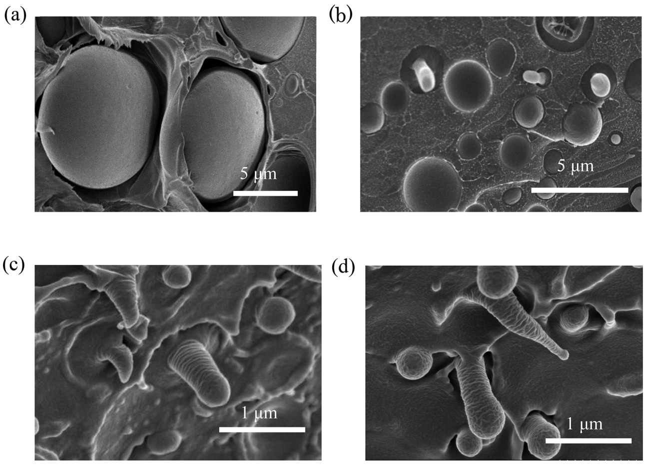

Figure 6. Representative SEM images of cryo-fractured polymer blends: (a) PET/PE (80/20), (b) PET/PE/MBCP-4k (80/20/0.5), (c) PET/PE/MBCP-4k (80/20/2), and (d) PET/PE/MBCP-7k (80/20/2).

components were also observed in the blend with 2 wt % of TBCP (Figure S19a). We assume that the TBCP can modestly reduce interfacial tension to reduce the droplet size of the PE phase during melt mixing, but it is not effective at promoting interfacial adhesion since both end blocks can be easily pulled out from the interface. The SEM images of the MBCP compatibilized blends (Figure 6b−d and Figure S19) show that the interfacial adhesion is significant as evidenced by the lack of clear gaps near the expected boundaries of the PET/PE phase. The adhesion appears to be so good that it is even difficult to identify the boundaries of the embedded spherical particles. In fact, the PE droplets were plastically deformed and elongated during the cryo-fracturing process, without detaching from the matrix; this is clearly one of the major operative mechanisms for improved ductility of blends with MBCPs. Considering that both blends with the addition of 2 wt % MBCP-4k and MBCP-7k have good adhesion enabling efficient stress transfer between two phases with a similar well-compatibilized structure whose droplet sizes are $<0.5\ \mu m$ (Figure 4), it is reasonable that both blends showed excellent mechanical properties without the significant difference. These structures were even observed in the blend with only 0.5 wt % MBCP (Figure 6b), again suggesting these new compatibilizers are highly efficient.

CONCLUSIONS

PET−PE MBCPs were synthesized for the first time through a coupling reaction between dihydroxy-terminated PET and PE precursors. The ability of these new MBCPs to improve interfacial adhesion and compatibilize immiscible polymer blends was investigated. Peel testing of laminated PET/PE films confirmed the poor adhesion between the neat components due to their immiscibility and relatively narrow interfaces. Placing PE−PET−PE TBCP interlayers in between the neat PET/PE layers did not significantly improve adhesion, while all MBCP interlayers dramatically increased peel strength by up to 2−3 orders of magnitude. In analogy to melt reprocessing mixed waste, the MBCPs also worked effectively as compatibilizers in PET/PE polymer blends. Adding only 0.5 wt % of MBCP to PET/PE (80/20) significantly reduced the size of the PE droplets in the PET matrix, while the strain at break increased over 30 times compared to neat blends. It was hypothesized that these improvements result from the efficient localization of MBCP at the interface. These results introduce the possibility of recycling or upcycling multicomponent PET/PE waste streams by direct melt blending with a preformed PET−PE MBCP; recycling processes involving waste streams that are impossible to physically separate, such as multilayer packaging film, or inconvenient to sort (e.g., PET bottles and caps) could both exploit this approach. Products where the MBCP additives are preloaded during initial manufacturing from virgin resin could make them ready for direct recycling after use. Finally, we anticipate this strategy could be generalized to other prevalent mixed-waste combinations, such as PET/polypropylene (PP).

ASSOCIATED CONTENT

Supporting Information

The Supporting Information is available free of charge at https://pubs.acs.org/doi/10.1021/acsami.9b20242.

Materials; experimental details; supporting calculations; NMR spectra; thermal analysis; SEC data; AFM images; SEM images; individual peel strength curves; individual stress−strain curves; SAXS data (PDF)

AUTHOR INFORMATION

Corresponding Authors

Kevin M. Miller − *Department of Chemistry, Murray State University, Murray, Kentucky 42071, United States;* orcid.org/0000-0001-5314-7477; Email: kmiller38@murraystate.edu

Christopher J. Ellison − *Department of Chemical Engineering and Materials Science, University of Minnesota, Minneapolis, Minnesota 55455, United States;* orcid.org/0000-0002-0393-2941; Email: cellison@umn.edu

Authors

Keiichiro Nomura − *Department of Chemical Engineering and Materials Science, University of Minnesota, Minneapolis, Minnesota 55455, United States; Chemicals Research Laboratories, Toray Industries Inc., Nagoya, Japan*

Xiayu Peng − *Department of Chemical Engineering and Materials Science, University of Minnesota, Minneapolis, Minnesota 55455, United States*

Hanim Kim − *Department of Chemical Engineering and Materials Science, University of Minnesota, Minneapolis, Minnesota 55455, United States*

Kailong Jin − *Department of Chemical Engineering and Materials Science, University of Minnesota, Minneapolis, Minnesota 55455, United States;* orcid.org/0000-0001-5428-3227

Hee Joong Kim − *Department of Chemical Engineering and Materials Science, University of Minnesota, Minneapolis, Minnesota 55455, United States;* orcid.org/0000-0001-6297-1636

Abigail F. Bratton − *Department of Chemistry, Murray State University, Murray, Kentucky 42071, United States*

Christopher R. Bond − *Department of Chemical Engineering and Materials Science, University of Minnesota, Minneapolis, Minnesota 55455, United States*

Amelia E. Broman − *Department of Chemical Engineering and Materials Science, University of Minnesota, Minneapolis, Minnesota 55455, United States*

Complete contact information is available at: https://pubs.acs.org/10.1021/acsami.9b20242

Author Contributions

K.N. and X.P. contributed equally. C.J.E. designed the concept. K.N., X.P., and H.K. performed the main part of experiments including sample preparation, characterization, SEM, and AFM. K.M.M., K.J., H.J.K., A.F.B., and A.E.B. synthesized and characterized block polymers. C.R.B. contributed to sample preparation and SEM. C.J.E. and K.M.M. guided the work. All authors worked on and commented on the manuscript.

Notes

The authors declare no competing financial interest.

ACKNOWLEDGMENTS

We thank Han Xiao for assistance in SEM. This work was supported by the NSF Center for Sustainable Polymers, CHE-1901635. This research was also partially supported by the University of Minnesota Industrial Partnership for Research in Interfacial and Materials Engineering (IPRIME) through

Toray's membership and their participation in the Industrial Fellows Program. Parts of this work were performed at the University of Minnesota College of Science and Engineering Characterization Facility, which receives partial support from NSF through the MRSEC program. The Table of Contents graphic is created by John Beumer with the NSF Center for Sustainable Polymers.

■ REFERENCES

(1) Geyer, R.; Jambeck, J. R.; Law, K. L. Production, Use, and Fate of All Plastics Ever Made. *Sci. Adv.* **2017**, *3* (7), No. e1700782.

(2) Barnes, D. K. A.; Galgani, F.; Thompson, R. C.; Barlaz, M. Accumulation and Fragmentation of Plastic Debris in Global Environments. *Philos. Trans. R. Soc., B* **2009**, *364* (1526), 1985−1998.

(3) Jambeck, J. R.; Geyer, R.; Wilcox, C.; Siegler, T. R.; Perryman, M.; Andrady, A.; Narayan, R.; Law, K. L. Plastic Waste Inputs from Land into the Ocean. *Science (Washington, DC, U. S.)* **2015**, *347* (6223), 768−771.

(4) Albertsson, A.-C.; Hakkarainen, M. Designed to Degrade. *Science (Washington, DC, U. S.)* **2017**, *358* (6365), 872−873.

(5) Feig, V. R.; Tran, H.; Bao, Z. Biodegradable Polymeric Materials in Degradable Electronic Devices. *ACS Cent. Sci.* **2018**, *4* (3), 337−348.

(6) Garcia, J. M.; Robertson, M. L. The Future of Plastics Recycling. *Science (Washington, DC, U. S.)* **2017**, *358* (6365), 870−872.

(7) USEPA. Plastic, 2015. https://archive.epa.gov/epawaste/conserve/tools/warm/pdfs/Plastics.pdf.

(8) Morris, B. A. Appendix B - Examples of Flexible Packaging Film Structures. In *The Science and Technology of Flexible Packaging*; Morris, B. A., Ed.; William Andrew Publishing: Oxford, 2017; pp 697−709.

(9) Uehara, G. A.; França, M. P.; Canevarolo Junior, S. V. Recycling Assessment of Multilayer Flexible Packaging Films Using Design of Experiments. *Polim.: Cienc. Tecnol.* **2015**, *25* (4), 371−381.

(10) Zheng, Y.; Guerra, S. M.; Hansen, S. E.; Walther, B. W. Resin for Use as Tie Layers in Multilayer Films and Multilayer Films Comprising the Same. International Patent WO2018/063578, 2018.

(11) Pucci, M. S.; Whaley, P. D.; Opacich, M. L. Adhesive Compositions, Articles Including the Adhesive Compositions, and Methods Thereof. International Patent WO2017/210423, 2017.

(12) Dalgewicz, E. J., III Multi-Layered Thermoplastic Container. U.S. Patent US 6,773,735, 2004.

(13) Ebeling, T.; Norek, S.; Hasan, A.; Hiltner, A.; Baer, E. Effect of a Tie Layer on the Delamination Toughness of Polypropylene and Polyamide-66 Microlayers. *J. Appl. Polym. Sci.* **1999**, *71* (9), 1461−1467.

(14) Morris, B. A. Effect of Process and Material Parameters on Interlayer Peel Strength in Coextrusion Coating, Film Casting and Film Blowing. *J. Plast. Film Sheeting* **2010**, *26* (4), 343−376.

(15) Birch, N. P.; Liu, K.; Mun, S. C.; Ghazaryan, G.; Senger, C. T.; Ellison, C. J.; Macosko, C. W.; Peterson, T. H.; Mukhopadhyay, S.; Thurber, C. M. Accelerating the Coupling of Maleated Polyolefins with Polyesters via Tin Compounds. *Macromolecules* **2019**, *52*, 8359.

(16) Yang, S.; Gupta, M. C. Surface Modification of Polyethyleneterephthalate by an Atmospheric-Pressure Plasma Source. *Surf. Coat. Technol.* **2004**, *187* (2−3), 172−176.

(17) Akishev, Y.; Grushin, M.; Dyatko, N.; Kochetov, I.; Napartovich, A.; Trushkin, N.; Minh Duc, T.; Descours, S. Studies on Cold Plasma-Polymer Surface Interaction by Example of PP- and PET-Films. *J. Phys. D: Appl. Phys.* **2008**, *41* (23), 235203.

(18) Wolf, R.; Sparavigna, A. C. Role of Plasma Surface Treatments on Wetting and Adhesion. *Engineering* **2010**, *02* (06), 397−402.

(19) Sapieha, S.; Cerny, J.; Klemberg-Sapieha, J. E.; Martinu, L. Corona versus Low Pressure Plasma Treatment: Effect on Surface Properties and Adhesion of Polymers. *J. Adhes.* **1993**, *42* (1−2), 91−102.

(20) Kaiser, K.; Schmid, M.; Schlummer, M. Recycling of Polymer-Based Multilayer Packaging: A Review. *Recycling* **2018**, *3* (1), 1.

(21) Morris, B. A. 1 - Introduction. In *The Science and Technology of Flexible Packaging*; Morris, B. A., Ed.; William Andrew Publishing: Oxford, 2017; pp 3−21.

(22) Paul, D. R.; Newman, S. *Polymer Blends*, 1st ed.; Academic Press: New York, 1978.

(23) Lee, M. S.; Lodge, T. P.; Macosko, C. W. Can Random Copolymers Serve as Effective Polymeric Compatibilizers? *J. Polym. Sci., Part B: Polym. Phys.* **1997**, *35* (17), 2835−2842.

(24) Bates, F. S.; Hillmyer, M. A.; Lodge, T. P.; Bates, C. M.; Delaney, K. T.; Fredrickson, G. H. Multiblock Polymers: Panacea or Pandora's Box? *Science (Washington, DC, U. S.)* **2012**, *336* (6080), 434−440.

(25) Ruzette, A.-V.; Leibler, L. Block Copolymers in Tomorrow's Plastics. *Nat. Mater.* **2005**, *4* (1), 19−31.

(26) Xu, Y.; Thurber, C. M.; Lodge, T. P.; Hillmyer, M. A. Synthesis and Remarkable Efficacy of Model Polyethylene-Graft -Poly(Methyl Methacrylate) Copolymers as Compatibilizers in Polyethylene/Poly(Methyl Methacrylate) Blends. *Macromolecules* **2012**, *45* (24), 9604−9610.

(27) Lohse, D. J.; Datta, S.; Kresge, E. N. Graft Copolymer Compatibilizers for Blends of Polypropylene and Ethylene-Propylene Copolymers. *Macromolecules* **1991**, *24* (2), 561−566.

(28) Zhu, Y.; Ma, Z.; Li, Y.; Cui, J.; Jiang, W. Monte Carlo Simulation of the Compatibility of Graft Copolymer Compatibilized Two Incompatible Homopolymer Blends: Effect of Graft Structure. *J. Appl. Polym. Sci.* **2007**, *105* (3), 1591−1596.

(29) Iniguez, C. G.; Michel, E.; Gonzalez-Romero, V. M.; Gonzalez-Nunez, R. Morphological Stability of Postconsumer PET/HDPE Blends. *Polym. Bull.* **2000**, *45* (3), 295−302.

(30) Barlow, J. W.; Paul, D. R. Mechanical Compatibilization of Immiscible Blends. *Polym. Eng. Sci.* **1984**, *24* (8), 525−534.

(31) Traugott, T. D.; Barlow, J. W.; Paul, D. R. Mechanical Compatibilization of High Density Polyethylene−Poly(Ethylene Terephthalate) Blends. *J. Appl. Polym. Sci.* **1983**, *28* (9), 2947−2959.

(32) Natarajan, K.; Arjunan, P.; Elwood, D. Impact Modified Polyester Blends with Improved Polymer Compatibility. U.S. Patent US5296550, 1994.

(33) Glanzstoff, A. G. A Process for the Production of High-Impact Injection Mouldings from Polyethylene Terephthalate. British Patent GB1091256, 1967.

(34) Sambaru, P.; Jabarin, S. A. Properties and Morphology of Oriented Ternary Blends of Poly(Ethylene Terephthalate), High Density Polyethylene, and Compatibilizing Agent. *Polym. Eng. Sci.* **1993**, *33* (13), 827−837.

(35) Carté, T. L.; Moet, A. Morphological Origin of Super Toughness in Poly(Ethylene Terephthalate)/Polyethylene Blends. *J. Appl. Polym. Sci.* **1993**, *48* (4), 611−624.

(36) Zhang, H.; Zhang, Y.; Guo, W.; Xu, D.; Wu, C. Thermal Properties and Morphology of Recycled Poly(Ethylene Terephthalate)/Maleic Anhydride Grafted Linear Low-density Polyethylene Blends. *J. Appl. Polym. Sci.* **2008**, *109* (6), 3546−3553.

(37) Coltelli, M.-B.; Harrats, C.; Aglietto, M.; Groeninckx, G. Influence of Compatibilizer Precursor Structure on the Phase Distribution of Low Density Poly(Ethylene) in a Poly(Ethylene Terephthalate) Matrix. *Polym. Eng. Sci.* **2008**, *48* (7), 1424−1433.

(38) Zhang, Y.; Zhang, H.; Guo, W.; Wu, C. Effects of Different Types of Polyethylene on the Morphology and Properties of Recycled Poly(Ethylene Terephthalate)/Polyethylene Compatibilized Blends. *Polym. Adv. Technol.* **2011**, *22* (12), 1851−1858.

(39) Kalfoglou, N. K.; Skafidas, D. S.; Kallitsis, J. K.; Lambert, J. C.; Van der Stappen, L. Comparison of Compatibilizer Effectiveness for PET/HDPE Blends. *Polymer* **1995**, *36* (23), 4453−4462.

(40) Pietrasanta, Y.; Robin, J.; Torres, N.; Boutevin, B. Reactive Compatibilization of HDPE/PET Blends by Glycidyl Methacrylate Functionalized Polyolefins. *Macromol. Chem. Phys.* **1999**, *200* (1), 142−149.

(41) Kim, D.-H.; Park, K.-Y.; Kim, J.-Y.; Suh, K.-D. Improved Compatibility of High-Density Polyethylene/Poly(Ethylene Tereph-

thalate) Blend by the Use of Blocked Isocyanate Group. *J. Appl. Polym. Sci.* **2000**, *78* (5), 1017−1024.

(42) Guerrero, C.; Lozano, T.; González, V.; Arroyo, E. Properties and Morphology of Poly(Ethylene Terephthalate) and High-Density Polyethylene Blends. *J. Appl. Polym. Sci.* **2001**, *82* (6), 1382−1390.

(43) Lusinchi, J. M.; Boutevin, B.; Torres, N.; Robin, J. J. In Situ Compatibilization of HDPE/PET Blends. *J. Appl. Polym. Sci.* **2001**, *79* (5), 874−880.

(44) Pluta, M.; Bartczak, Z.; Pawlak, A.; Galeski, A.; Pracella, M. Phase Structure and Viscoelastic Properties of Compatibilized Blends of PET and HDPE Recyclates. *J. Appl. Polym. Sci.* **2001**, *82* (6), 1423−1436.

(45) Pracella, M.; Rolla, L.; Chionna, D.; Galeski, A. Compatibilization and Properties of Poly(Ethylene Terephthalate)/Polyethylene Blends Based on Recycled Materials. *Macromol. Chem. Phys.* **2002**, *203* (10−11), 1473−1485.

(46) Pawlak, A.; Morawiec, J.; Pazzagli, F.; Pracella, M.; Galeski, A. Recycling of Postconsumer Poly(Ethylene Terephthalate) and High-Density Polyethylene by Compatibilized Blending. *J. Appl. Polym. Sci.* **2002**, *86* (6), 1473−1485.

(47) Todd, A. D.; McEneany, R. J.; Topolkaraev, V. A.; Macosko, C. W.; Hillmyer, M. A. Reactive Compatibilization of Poly(Ethylene Terephthalate) and High-Density Polyethylene Using Amino-Telechelic Polyethylene. *Macromolecules* **2016**, *49* (23), 8988−8994.

(48) Eastwood, E. A.; Dadmun, M. D. Multiblock Copolymers in the Compatibilization of Polystyrene and Poly(Methyl Methacrylate) Blends: Role of Polymer Architecture. *Macromolecules* **2002**, *35* (13), 5069−5077.

(49) Eagan, J. M.; Xu, J.; Di Girolamo, R.; Thurber, C. M.; Macosko, C. W.; La Pointe, A. M.; Bates, F. S.; Coates, G. W. Combining Polyethylene and Polypropylene: Enhanced Performance with PE/*i*PP Multiblock Polymers. *Science (Washington, DC, U. S.)* **2017**, *355* (6327), 814−816.

(50) Xu, J.; Eagan, J. M.; Kim, S.-S.; Pan, S.; Lee, B.; Klimovica, K.; Jin, K.; Lin, T.-W.; Howard, M. J.; Ellison, C. J.; Lapointe, A. M.; Coates, G. W.; Bates, F. S. Compatibilization of Isotactic Polypropylene (*i*PP) and High-Density Polyethylene (HDPE) with *i*PP−PE Multiblock Copolymers. *Macromolecules* **2018**, *51* (21), 8585−8596.

(51) Lee, I.; Panthani, T. R.; Bates, F. S. Sustainable Poly(Lactide-b-Butadiene) Multiblock Copolymers with Enhanced Mechanical Properties. *Macromolecules* **2013**, *46* (18), 7387−7398.

(52) Panthani, T. R.; Bates, F. S. Crystallization and Mechanical Properties of Poly(l-Lactide)-Based Rubbery/Semicrystalline Multiblock Copolymers. *Macromolecules* **2015**, *48* (13), 4529−4540.

(53) Pitet, L. M.; Amendt, M. A.; Hillmyer, M. A. Nanoporous Linear Polyethylene from a Block Polymer Precursor. *J. Am. Chem. Soc.* **2010**, *132* (24), 8230−8231.

(54) Wang, Y.; Hillmyer, M. A. Hydroxy-Telechelic Poly(Ethylene-Co-Isobutylene) as a Soft Segment for Thermoplastic Polyurethanes. *Polym. Chem.* **2015**, *6* (38), 6806−6811.

(55) Wu, S. Chain Structure and Entanglement. *J. Polym. Sci., Part B: Polym. Phys.* **1989**, *27* (4), 723−741.

(56) Cole, P. J.; Cook, R. F.; Macosko, C. W. Adhesion between Immiscible Polymers Correlated with Interfacial Entanglements. *Macromolecules* **2003**, *36* (8), 2808−2815.

(57) Fetters, L. J.; Lohse, D. J.; Richter, D.; Witten, T. A.; Zirkel, A. Connection between Polymer Molecular Weight, Density, Chain Dimensions, and Melt Viscoelastic Properties. *Macromolecules* **1994**, *27* (17), 4639−4647.

(58) Zeng, Y.; López-Barrón, C. R.; Kang, S.; Eberle, A. P. R.; Lodge, T. P.; Bates, F. S. Effect of Branching and Molecular Weight on Heterogeneous Catalytic Deuterium Exchange in Polyolefins. *Macromolecules* **2017**, *50* (17), 6849−6860.

(59) Hameed, T.; Hussein, I. A. Melt Miscibility and Mechanical Properties of Metallocene LLDPE Blends with HDPE: Influence of Mw of LLDPE. *Polym. J.* **2006**, *38* (11), 1114−1126.

(60) Hussein, I. A. Influence of Composition Distribution and Branch Content on the Miscibility of M-LLDPE and HDPE Blends: Rheological Investigation. *Macromolecules* **2003**, *36* (6), 2024−2031.

(61) Russell, T. P.; Anastasiadis, S. H.; Menelle, A.; Felcher, G. P.; Satija, S. K. Segment Density Distribution of Symmetric Diblock Copolymers at the Interface between Two Homopolymers As Revealed by Neutron Reflectivity. *Macromolecules* **1991**, *24* (7), 1575−1582.

(62) Berry, G. C.; Fox, T. The Viscosity of Polymers and Their Concentrated Solutions. *Fortschritte der Hochpolym.* **1968**, *5/3*, 261−357.

(63) Zhang, J.; Lodge, T. P.; Macosko, C. W. Models for Adhesion at Weak Polymer Interfaces. *J. Polym. Sci., Part B: Polym. Phys.* **2009**, *47* (23), 2313−2319.

(64) Macosko, C. W.; Guégan, P.; Khandpur, A. K.; Nakayama, A.; Marechal, P.; Inoue, T. Compatibilizers for Melt Blending: Premade Block Copolymers. *Macromolecules* **1996**, *29* (17), 5590−5598.

(65) Noolandi, J. Multiblock Copolymers as Polymeric Surfactants: Are "Pancakes" Better than "Dumbbells"? *Makromol. Chem., Theory Simul.* **1992**, *1* (5), 295−298.

(66) Balazs, A. C.; Siemasko, C. P.; Lantman, C. W. Monte Carlo Simulations for the Behavior of Multiblock Copolymers at a Penetrable Interface. *J. Chem. Phys.* **1991**, *94* (2), 1653−1663.

(67) Corsi, A.; Milchev, A.; Rostiashvili, V. G.; Vilgis, T. A. Localization of a Multiblock Copolymer at a Selective Interface: Scaling Predictions and Monte Carlo Verification. *J. Chem. Phys.* **2005**, *122* (9), 094907.